

Birefringent elastomers with Multiple Stimuli-Responses

Yiyang Gao

Xi'an Jiaotong University

Danqi Sun

School of Aerospace Engineering, Xi'an Jiaotong University

Jing Chen

School of Chemistry, Xi'an Jiaotong University

Lei Shi

School of Materials, Sun Yat-sen University

Xinyu Da

School of Chemistry, Xi'an Jiaotong University

Haoyu Guo

School of Aerospace Engineering, Xi'an Jiaotong University

Kai Xi

University of Cambridge <https://orcid.org/0000-0003-0508-7910>

Dongyang Zhang

School of Chemistry, Xi'an Jiaotong University

Ting Gao

Chengdu Galaxy Power Co., Ltd

Guoxin Gao

Xi'an Jiaotong University

Tongqing Lu

Xi'an Jiaotong University <https://orcid.org/0000-0002-1333-7978>

Shujiang Ding (✉ dingsj@mail.xjtu.edu.cn)

School of Chemistry, Xi'an Jiaotong University

Article

Keywords:

Posted Date: December 15th, 2021

DOI: <https://doi.org/10.21203/rs.3.rs-1150417/v1>

License:  This work is licensed under a Creative Commons Attribution 4.0 International License.

[Read Full License](#)

Abstract

Currently, even though birefringent soft materials have attracted considerable attention for many sensors and optical devices, it is still difficult for most of them to achieve multiple responses. Herein, we have designed a multiple-responding birefringent elastomer with high birefringence but low modulus by using 2-phenoxy-ethanoacrylate (PHEA) as monomer and 4-cyano-4'pentylbiphenyl as solvent. The excellent transparency (~90%) exhibited by the designed birefringent elastomer allowed us to observe the change of interference color. The obtained birefringent elastomer not only can be used as a photoelastic strain sensor with high sensitivity and fast response but also show a very sensitive response to heat, particularly in the range of the human body temperature. More interestingly, it shows excellent dielectric properties with a strong correlation between the interference color and the applied electric field, which allows easily writing and erasing the encrypted information. These unique multi-signal response features of our obtained birefringent elastomer shed light on the multiple information encryptions, the anti-counterfeiting, and the multifunctional sensors.

Introduction

The interference color produced by birefringence is a structural color, which is different from the pigments used in daily life. This structural color possesses a wider color gamut, higher brightness. And importantly, it is non-toxic and harmless. Therefore, the interference color is a kind of ideal “healthy color”¹⁻⁸. Flexible materials with specific structures will change the anisotropy of the internal segment under stress, thereby changing the birefringence. As a result, significant changes of the interference color can be observed when placing the birefringent materials between the crossed or parallel polarizers⁹⁻¹⁵. This color change can be controlled accurately via changing the optical path difference, which, in a responsive material, can be changed by stimuli such as electric field¹⁶⁻¹⁸, magnetic field¹⁹, stress field²⁰ and so on. The structural color produced by the birefringence of light is pollution-free and can be stored for a long time²¹⁻²³. Therefore, it could be widely used in many fields such as anti-counterfeiting and information encryption²⁴⁻³⁰.

Recently, the structural color produced by the birefringence of light in polymer elastomer materials has inspired new optical applications. Xie *et al.* implemented a digital photothermal mechanism enabled by laser printing to encode stress with polymers³¹. The stress was invisible under regular light but could be visualized under polarized light due to the birefringence. This mechanism can be well applied in the information security field. MacLachlan *et al.* introduced cellulose nanocrystals in poly(ethyl acrylate) (PEA) elastomer and successfully identify the relationship between the change in the interference color with the level and the direction of the applied stress³². Although cellulose nanocrystals/PEA composites showed qualitative results using the birefringence in elastomer to sense the mechanical strain, more precise and quantitative data are necessary before their practical application. The sensitivity of their composites is so low that it needs big deformation (strain) to produce distinct color differences. More importantly, the composite showed a nonlinear relationship between stress and strain, as it is for liquid

crystal elastomers (LCEs), which is known as soft elasticity. This soft elasticity makes it challenging to correlate the interference color changes with the elongation, particularly at low and high-stress values. Gleeson et al. developed an acrylate-based anisotropic elastomer with a nonlinear relationship of strain with the induced birefringence and high strain-optic coefficients³³. They used it for photoelastic strain sensors. However, little is known about the response of the acrylate-based anisotropic elastomer strain sensor under other stimuli.

Nowadays, there is an ever-increasing trend to develop multiple stimuli-responsive materials that can simultaneously monitor more physical or/and chemical changes in their surroundings. Inspired by the above-reported literature, we designed a birefringent elastomer to realize three kinds of physical field changes: stress, temperature, and electric field. In order to endow the multiple stimuli-responsive functions, during the fabrication of our birefringent elastomer, we chose 2-phenoxy-ethanoacrylate (PHEA) as the monomer due to its high refractive index. In addition, the liquid crystal molecule (4-cyano-4'-pentylbiphenyl) was adopted as the solvent thanks to its easy orientation under external fields. Consequently, our designed birefringent elastomer delivers the characteristics of low modulus and high birefringence. It can transmit different information by changing interference colors following high response sensitivity. Meanwhile, the solvent imparts unique dielectric properties to the elastomer to change the birefringence under the electric field. As a purely elastic material, under constant external field, it will not undergo stress relaxation and the interference color will not change. The color information in the birefringent elastomer can be stored for a long time. Therefore, our designed birefringent elastomer holds a great promise in multiple information encryption, flexible multifunctional sensors and flexible display devices.

Results And Discussion

2.1 Design and preparation of the birefringent elastomer

In order to prepare an elastomer with a high birefringence effect, we chose PHEA as the monomer, which has a refractive index as high as 1.52. Due to the existence of the rigid phenyl group, the internal structure of the elastomers can be oriented under applied stress easily. In addition, we chose 4-cyano-4'pentylbiphenyl, which has a biphenyl structure, as the solvent. As shown in **Figure 1c**, this solvent is a common liquid crystal molecule with a rod-like structure. The polarizability of the two ends of this molecule is very different, making it oriented easily in the electric field. Adjusting the external electronic field also can change the degree of anisotropy of the birefringent elastomer. As schematized in **Figure 1a**, the initial birefringent elastomer is isotropic. Nevertheless, under stress stretching, the polymer chain segments of the elastomer will reorient along the direction of stretching, resulting in a temporary anisotropy. Simultaneously, the solvent molecules will rotate under the drive of polymer chains, further intensifying the anisotropy of the birefringent elastomer. Additionally, temperature also can affect the elastomer anisotropy via changing the thermal motion of molecule. Correspondingly, if placed in the electric field, the solvent molecules will be arranged orderly under the action of electric field and make the elastomer produce anisotropy. Benefiting from the similar molecule structure feature, PHEA monomer and

as-adopted liquid crystal solvent exhibit excellent compatibility. As shown in **Figure 1b**, the transmittance of this birefringent elastomer in the visible light is over 90% and hardly changes with the solvent content of 20%, 40% and 60%, presenting excellent transparency. **Figure 1d** displays the color of the birefringent elastomer in the stretched state as seen through the polarizer and polarized microscope. The upper picture shows the bright field (the polarization directions of the two polarizers are parallel), and the lower picture shows the dark field (the polarization directions of the two polarizers are perpendicular to each other). The colors of the bright field and the dark field are complementary. We further conducted a series of experiments to qualitatively assess the relationship between the direction of the anisotropy and the polarization. **Figure S1** (see Supporting Information) is the photographs and the polarizing microscope pictures of the elastomer stretched in different directions. When the stretching direction of the elastomer is parallel or perpendicular to the polarization direction, no color can be seen through the polarizer. Rotating the stretched elastomer samples, their color emerges gradually, reaching maximum brightness at 45° and 135° relative to the polarization. When the direction of anisotropy is parallel or perpendicular to the polarization direction, the incident light beam either completely passes through the sample or is completely blocked without birefringence. Since birefringence is maximum at 45°, this angle was chosen in our following experiments unless otherwise specified. We also tested the light transmittance of the elastomer after attaching the polarizers. As shown in **Figure S2** (see Supporting Information), the transparency of the elastomer drops from 20% to 0% at wavelength ranges from 750 nm to 530 nm. The transparency rises rapidly at a lower wavelength, reaching a peak at 430 nanometers, with a transparency of 72%. The digital photo (inset of **Figure S2**) also shows that the elastomer's color under polarized light is purple.

2.2 Test and calculation of mechanical response of birefringent elastomer

We then conducted a series of experiments aiming to determine the optimum elastomer composition. First, we tested the mechanical properties of birefringent elastomers with different solvent contents. As shown in Figure 2a, with the increasing of liquid crystal (4-cyano-4'-pentylbiphenyl) contents from 20% to 60%, the elongations at break of the birefringent elastomers increase gradually, but their tensile strengths decrease rapidly. At the same time, we photographed the interference colors change of birefringent elastomers with different solvent content during the stretching process. As shown in **Figure 2b**, the change rate of interference colors is accelerated upon the solvent content gradually increasing from 0% to 40%. But once the solvent content is over 40%, the change rate of interference colors will slow down. For example, in the absence of liquid crystal solvent, the birefringent elastomer presents a tawny interference color with a strain of 40%. However, it only needs 25% stretch strain to present this color for the birefringent elastomer with 40% of solvent. Further increasing the solvent content to 60%, a stretch strain of 50% is necessary to maintain the tawny interference colors again. The possible reason should be that the greater the density of the polymer network, the greater the degree of birefringence. But after reaching a certain critical density, the change of the birefringence with the polymer network will tend to be gentle. Therefore, we reduce the solid content and fill the small liquid crystal molecules as the solvent. The benzene rings in the liquid crystal molecule and the monomer have π - π stacking interaction. When some stress is applied onto the polymer network, the deformation will drive the deflection of the liquid

crystal. The rotation of the liquid crystal has a considerable contribution to the birefringence. However, with the further increase of the liquid crystal content, the density of the polymer network is severely reduced, and the birefringence provided by the polymer will be greatly reduced. At the same time, the interaction between the chain segment and the small liquid crystal molecules will also be reduced, and the deformation of the network is challenging to drive the deflection of the liquid crystal, so the degree of birefringence will decrease instead.

In order to quantitatively study the relationship between birefringence and solvent content, we performed simple theory calculations. We compared the colors of our birefringent elastomer depicted in **Figure 2b** with Michel-Levy Birefringence Chart (**Figure S3**) and drew the curves of optical path difference versus strain (**Figure 2c**). The optical path difference Δn can be calculated according to the Eq(1).³⁴⁻³⁷

$$\Delta n = CN (\lambda_1^2 - \lambda_2^2) \quad (1)$$

where C is the birefringence coefficient, N is the number of segments and λ is the strain. In the case of

uniaxial stretching, $\lambda_1 = \lambda$, $\lambda_2 = \frac{1}{\sqrt{\lambda}}$. Therefore,

$$\Delta n = CN (\lambda^2 - \frac{1}{\lambda}) \quad (2)$$

In a small deformation range, Δn has a linear relationship with λ , and the slope of the curve in **Figure 2c** can be approximated as a constant CN. The modulus (μ) of the elastomer could be calculated according to $\mu = NkT$. Herein k is Boltzmann constant and T is room temperature. So birefringence coefficient (C) should be obtained according to Eq(3).

$$C = \frac{\Delta n kT}{N(\lambda^2 - \frac{1}{\lambda})} \quad (3)$$

We adopt the sample containing 40% solvent content as an example (maximum slope), CN is approximately 518×10^{-6} . The final value of C is calculated to be 1.91×10^{-26} . The value is much larger than polyacrylamide (PAAm) hydrogel ($C = 7.7 \times 10^{-30}$) and poly (N,N'-dimethylacrylamide) (PDMA) hydrogel ($C = 12.2 \times 10^{-30}$)^{34, 38}.

Next, we tested the color evolution of our designed birefringent elastomer during the entire stretching process. **Figure S4** (see Supporting Information) shows the color change of the birefringent elastomers during the stretching progress. The extracted RGB values of the color are in **Table S1** (see Supporting Information), and the corresponding CIE-Yxy values are listed in **Table S2** (see Supporting Information), which then used to plot the CIE-1931 color space (**Figure 2d**). Obviously, the interference colors have an extensive range, especially in the blue area. It can also be seen that the green and red interference colors

coordinate at the CIE-1931 have small areas, which we believe has nothing to do with the nature of the birefringent elastomer itself. The limited area of green color is because the screens that provide polarized light only support the sRGB color gamut (yellow dotted line). Interestingly, the developed elastomer can also be used to visualize the stress distributions and detect any defects within the matrix, as can be seen in **Movie S1** (see Supporting Information), implying a great application promise of our developed elastomer as a structural material with spontaneous defect detection functionality or as a functional coating on other substrates. Subsequently, we conducted a stress relaxation experiment on the birefringent elastomer via stretching the birefringent elastomer to 50% strain and maintaining it for a while (**Figure S5**, see Supporting Information). As anticipated, the stress hardly attenuates during the relaxation process. Meanwhile, we also tracked the change of interference colors and presented it in **Movie S2** (see Supporting Information). Further, we evaluated the tensile recovery performance of the birefringent elastomer again. As presented in **Figure 2e**, when the tensile samples were stretched to 10%, 20%, 40%, 60% and 80% at the stretch speed of 30 mm min^{-1} , respectively, the strain could recover rapidly to their initial state once the stretch stress is withdrawn. The stretch and recovery profiles overlap very well and no distinct stress-strain hysteresis appears between the couple curves, indicating the excellent elasticity reversibility of our designed birefringent elastomer. Correspondingly, the change of interference colors is also recorded in **Movie S3** (see Supporting Information). Therefore, the developed birefringent elastomer can almost be regarded as a purely elastic material with superb elasticity. Subsequently, we further carried out 100 tensile recovery tests of the birefringent elastomer to demonstrate their anti-fatigue performance. As shown in **Figure S6** (see Supporting Information), the stress of the elastomer still has no obvious fatigue even after 100 stretch-recovery cycles and the residual stress even could be negligible.

Under controlling the solvent content to 40%, we systematically compared 4-cyano-4'-pentyl biphenyl with other common plasticizers such as propylene carbonate (PC), dimethyl phthalate (DMP), butyl benzyl phthalate (BBP) and tributyl citrate (TBC). As demonstrated in **Movie S4** (see Supporting Information), the birefringent elastomer with 4-cyano-4'pentyl biphenyl solvent reveals the clearest contrast of color changes among all the tested solvents, meaning that it owns the highest sensitivity to tensile load. Besides, the excellent compatibility between PHEA monomer and liquid crystal solvent has significantly improved mechanical properties with the highest elongation in all the tested elastomers (**Figure S7**).

2.3 Temperature response test of the birefringent elastomer

Temperature also has an essential influence on the interference colors of our designed birefringent elastomer. As well known, in the same strain, increasing temperature will accelerate the diffusion of liquid crystal molecules and improve the segmental motion ability of polymer matrix, thus greatly decreasing their anisotropy degree. In order to demonstrate such segmental motion change, we first tested the thermal performance of our prepared elastomers by using thermogravimetric analysis (TGA) and differential scanning calorimeter (DSC). As shown in **Figure 3a**, the pure polymer matrix hardly suffers from a great mass loss before $385\text{ }^{\circ}\text{C}$, demonstrating excellent thermal stability. Even after filling in 20% or 40% liquid crystal solvent, the thermal stability of our designed birefringent elastomer composites is

also excellent before 230 °C. Over 230 °C, the liquid crystal solvent will gradually volatilize and increase the rapid mass loss. Further increasing temperature to 385 °C will lead to sharp mass loss mainly due to the decomposition of the polymer backbone. Simultaneously, the DSC profiles also present that the glass temperatures of our polymer matrix and the liquid crystal solvent are -20 °C and -68 °C, respectively (**Figure 3b**). However, since the solvent is a liquid crystal molecule, it is easy to crystallize at low temperatures, usually exhibiting white color. Therefore, it is not recommended to use our birefringent elastomer at sub-zero temperatures. Then we further quantitatively tested the relationship between temperature and the interference colors of our birefringent elastomer and plotted the relevant color coordinates. **Figure 3c** shows the relationship between the temperature and the interference color for the birefringent elastomer sample with 2mm thick and 16 mm length elongated up to 20 mm. It can be seen that when the temperature gradually drops from 120 °C to 15 °C, the interference colors of the birefringent elastomer also change from orange to red, blue, pink and then green correspondingly, showing excellent temperature dependence. **Figure 3d** discloses that with the temperature increasing from 15 °C to 120 °C, the optical path difference (Δn) decreases quickly, especially in the low temperature area, thus demonstrating inuniform color changing the speed at different temperatures. Remarkably, near the human body temperature (35~40 °C), the contrast of the color changes is clearer. Therefore, our designed birefringent elastomer could also be used as the temperature sensor in clinical thermometers and the image processing in information encryption. Changing the temperature locally on a stretched elastomer could print a specific pattern observed under polarized light. **Figure 3e** shows a straightforward information encryption display. A copper seal with the emblem of Xi'an Jiaotong University was preheated and placed close to a stretched elastomer sample for a few seconds. As a result, no visible color change can be seen for the elastomer sample without the polarizer. However, the sample close to the hot copper seal presents distinguished interference color under the polarized light. Next, we further investigated the interference color change of our birefringent elastomers via putting them at 100 °C for 1h and then quenching them to room temperature again (**Figure 3f**). Interestingly, no distinct variation in the sample color under the same elongation can be observed under the polarized light. Correspondingly, the same results also can be confirmed if we put the samples in the cryogenic condition (-25 °C) and then heated them back to room temperature again. Remarkably, even stored in air for 6 months, the interference color of our birefringent elastomer is hardly different from its initial color, revealing superb environmental stability of our birefringent elastomer. The dynamic change of the interference color of our birefringent elastomer with the temperature is recorded in real-time in **Movie S5** (see Supporting Information). Coupled with the above-mentioned thermal and environmental stabilities, the encrypted information of our developed birefringent elastomer can be stored for a long time without any information loss.

2.4 Electric field response test of the birefringent elastomer

Finally, applying an electric field across birefringent elastomers can also change the interference color. The solvent in our developed birefringent elastomer, 4-cyano-4'-pentylbiphenyl, is one of the most common liquid crystal materials, inspiring us to design a new display device. We first tested the dielectric constant of the birefringent elastomers with different solvent contents. **Figures 4a** show that the dielectric

constants of the birefringent elastomer are 14, 16, 21, 28 and 43 at the frequency of 1000 Hz at the liquid crystal contents of 30%, 40%, 50%, 60% and 70%, respectively. Obviously, the dielectric constant of our birefringent elastomer is much higher than that of common elastomers (PDMS, VHB and most insulating gels), which means that our birefringent elastomer could be driven by an electric field easily. So we then investigated the interference color change of our elastomer under various electric field strengths. As shown in **Figure 4b**, the display device was constructed by sandwiching a piece of birefringent elastomer film containing 70% solvent content with the dimension of 25mm × 25 mm × 5 mm between two pieces of ITO conductive glasses. As a result, the randomly oriented small liquid crystal molecules will be rearranging themselves parallel to the electric field upon applying voltage. Simultaneously, compression stress (1N) will load onto the sample along the electric field to keep consistency. As a result, the middle part of the display device delivers green color (**Figure 4c**) when no electric field is applied. Upon increasing the applied voltage from 0 V to 8 kV, the color of the middle part of the elastomer changes from light green to yellow. The optical path difference of the voltage change process is also presented in **Figure 4d**. When the voltage is less than 4kV, the electric drive effect is small and the color changes slowly. When the voltage is larger than 4kV, the interference color changes significantly, and the slope of the curve in **Figure 4d** also increases rapidly. In addition, we also shot a video of the change in the interference color of the elastomer caused by applying electric field (**Movie S6**). Obviously, whether the voltage change is gradual or instantaneously, the display device had the same color at the same applied voltage, suggesting the birefringent elastomer can be used for real-time monitoring of high voltage loads.

In the end, we linked the signal responses of the three physical fields via putting our designed birefringent elastomer and ITO glasses on a heating plate with the loadings of 20 g, 50 g, and 100 g respectively on the ITO glass. As shown in **Figure S8a** (see Supporting Information), the main colors of the elastomer are yellow, pink, and blue, respectively. Then we applied the voltage of 5kV between ITO glasses. The main color under the three stresses becomes colorless, yellow, and orange, respectively. After that, we fixed the loading of 100 g unchanged and heated the elastomer to different temperatures. As shown in **Figure S8b** (see Supporting Information), the main colors of the elastomer at 50 °C, 60 °C and 70 °C were blue, purple, and orange, respectively. Then the voltage of 5 kV was applied, the colors of the birefringent elastomer are changed to purple, orange and yellow. It confirms that three physical fields can affect the interference color of our birefringent elastomer independently or together. Therefore, we can use the birefringent elastomer to encrypt information multiple times, and can also write and erase new information repeatedly.

Conclusions

In this work, we have successfully developed a new multiple response birefringent elastomer based on the combination of liquid crystal small molecule (4-cyano-4'pentylbiphenyl) and PHEA via a simple photo-curing process. The results show that the birefringence degree of elastomer can be controlled accurately by changing the ratio of monomer and solvent. The interference color of the birefringent elastomer is sensitive to the applied stress, temperature and electric fields. When the elastomer is used as a strain sensor, the interference colors can correspond to the elongation and change uniformly and continuously.

When the elastomer is considered as a temperature sensor, it could detect the changes quickly in the temperature range from 15 °C to 120 °C with relatively high sensitivity, especially around the human body temperature. Besides, the elastomer presented a swift response to the gradual and sudden voltage change under electric field. More importantly, the developed elastomer could detect simultaneous changes of a mixed stimulus. The response of this structural color is speedy, and the color has good stability and reversibility. Thus, it makes it possible to encrypt data that was only visible under the polarized light within the elastomer. Our work also showed the ability to write and erase encrypted information repeatedly. For this reason, this novel birefringent elastomer can be considered as an ideal material for anti-counterfeiting, information encryption, flexible display, and multifunctional sensors.

Declarations

Acknowledgements

This research was supported by the National Natural Science Foundation of China (No. 51973171), Natural Science Foundation of Shaanxi Province (No. 2019JM-175, 2021GXH-Z-075), Natural Science Basic Research Program of Shaanxi (No. 2020JC-09), Fundamental Research Funds for the Central Universities (xhj032021014-02)

Appendix A. Supporting information

The supporting information is available free of charge on the Publications website.

References

1. Jiang P, et al. Drawing High-Definition and Reversible Hydrogel Paintings with Grayscale Exposure. *ACS Appl. Mater. Inter.* **11**, 42586-42593 (2019).
2. Wang J, Wang Z, Song Z, Ren L, Liu Q, Ren L. Biomimetic Shape-Color Double-Responsive 4D Printing. *Adv. Mater. Technol.* **4**, 1900293 (2019).
3. Xu L, Feng Y, Yu D, Zheng Z, Chen X, Hong W. Recoverable Photolithographic Patterning for Polarized Display and Encryption. *Adv. Mater. Technol.* **5**, 2000373 (2020).
4. Chen D, et al. Drilling by light: ice-templated photo-patterning enabled by a dynamically crosslinked hydrogel. *Mater. Horizons* **6**, 1013-1019 (2019).
5. Fan W, et al. Iridescence-controlled and flexibly tunable retroreflective structural color film for smart displays. *Sci. Adv.* **5**, eaaw8775 (2019).
6. Clough JM, van der Gucht J, Kodger TE, Sprakel J. Cephalopod-Inspired High Dynamic Range Mechano-Imaging in Polymeric Materials. *Adv. Funct. Mater.* **30**, 2002716 (2020).

7. Niu W, et al. Photonic Vitrimer Elastomer with Self-Healing, High Toughness, Mechanochromism, and Excellent Durability based on Dynamic Covalent Bond. *Adv. Funct. Mater.* **31**, 2009017 (2021).
8. Zhang J, et al. Photonic Plasticines with Uniform Structural Colors, High Processability, and Self-Healing Properties. *Small* **17**, 2007426 (2021).
9. Huang H, et al. Liquid-Behaviors-Assisted Fabrication of Multidimensional Birefringent Materials from Dynamic Hybrid Hydrogels. *ACS Nano* **13**, 3867-3874 (2019).
10. Gray DG. Recent Advances in Chiral Nematic Structure and Iridescent Color of Cellulose Nanocrystal Films. *Nanomaterials* **6**, 213 (2016).
11. Ye D, et al. Ultrahigh Tough, Super Clear, and Highly Anisotropic Nanofiber-Structured Regenerated Cellulose Films. *ACS Nano* **13**, 4843-4853 (2019).
12. Liu Y, Wu P. Bioinspired Hierarchical Liquid-Metacrystal Fibers for Chiral Optics and Advanced Textiles. *Adv. Funct. Mater.* **30**, 2002193 (2020).
13. Boott CE, Tran A, Hamad WY, MacLachlan MJ. Cellulose Nanocrystal Elastomers with Reversible Visible Color. *Angew. Chem. Int. Ed.* **59**, 226-231 (2020).
14. Kose O, Boott CE, Hamad WY, MacLachlan MJ. Stimuli-Responsive Anisotropic Materials Based on Unidirectional Organization of Cellulose Nanocrystals in an Elastomer. *Macromolecules* **52**, 5317-5324 (2019).
15. Mredha MTI, Le HH, Van Tron T, Trtik P, Cui J, Jeon I. Anisotropic tough multilayer hydrogels with programmable orientation. *Mater. Horizons* **6**, 1504-1511 (2019).
16. Luk YY, Abbott NL. Surface-driven switching of liquid-crystals using redox-active groups on electrodes. *Science* **301**, 623-626 (2003).
17. Qu D, Zussman E. Electro-responsive Liquid Crystalline Nanocelluloses with Reversible Switching. *J Phys Chem. Lett.* **11**, 6697-6703 (2020).
18. Zhao P, Cai Y, Liu C, Ge D, Li B, Chen H. Study on the bio-inspired electrochromic device enabled via dielectric elastomer actuator. *Opt. Mater.* **111**, 110569 (2021).
19. Ding B, et al. Giant magneto-birefringence effect and tuneable colouration of 2D crystal suspensions. *Nat. Commun.* **11**, 3725 (2020).
20. Chen G, Hong W. Mechanochromism of Structural-Colored Materials. *Adv. Opt. Mater.* **8**, 2000984 (2020).
21. Liu C, Fan Z, Tan Y, Fan F, Xu H. Tunable Structural Color Patterns Based on the Visible-Light-Responsive Dynamic Diselenide Metathesis. *Adv. Mater.* **32**, 1907569 (2020).

22. Chen J, Xu L, Yang M, Chen X, Chen X, Hong W. Highly Stretchable Photonic Crystal Hydrogels for a Sensitive Mechanochromic Sensor and Direct Ink Writing. *Chem. Mat.* **31**, 8918-8926 (2019).
23. Wang X, et al. Structural Colors by Synergistic Birefringence and Surface Plasmon Resonance. *ACS Nano* **14**, 16832-16839 (2020).
24. Chen R, Feng D, Chen G, Chen X, Hong W. Re-Printable Chiral Photonic Paper with Invisible Patterns and Tunable Wettability. *Adv. Funct. Mater.* **31**, 2009916 (2021).
25. Zhou Q, et al. Multimodal and Covert-Overt Convertible Structural Coloration Transformed by Mechanical Stress. *Adv. Mater.* **32**, 2001467 (2020).
26. Zhao F, Li G, Ji X, Fu Y, Qin M, Yuan Z. Mechano-optical response of micellar hydrogel films. *Appl. Surf. Sci.* **539**, 148228 (2021).
27. Tao L, et al. Wavelength-tunable linearly polarized luminescence film constructed using a highly efficient luminescent liquid crystal with stimuli-responsive property. *J. Mater. Chem. C* **8**, 16561-16568 (2020).
28. Hong W, Yuan Z, Chen X. Structural Color Materials for Optical Anticounterfeiting. *Small* **16**, 1907626 (2020).
29. Zhang Z-L, et al. Chameleon-Inspired Variable Coloration Enabled by a Highly Flexible Photonic Cellulose Film. *ACS Appl. Mater. Inter.* **12**, 46710-46718 (2020).
30. Yang Y, et al. Modular Nanocomposite Films with Tunable Physical Organization of Cellulose Nanocrystals for Photonic Encryption. *Adv. Opt. Mater.* **8**, 2000547 (2020).
31. Zhang G, Peng W, Wu J, Zhao Q, Xie T. Digital coding of mechanical stress in a dynamic covalent shape memory polymer network. *Nat. Commun.* **9**, 4002 (2018).
32. Kose O, Tran A, Lewis L, Hamad WY, MacLachlan MJ. Unwinding a spiral of cellulose nanocrystals for stimuli-responsive stretchable optics. *Nat. Commun.* **10**, 510 (2019).
33. Mistry D, et al. Isotropic Liquid Crystal Elastomers as Exceptional Photoelastic Strain Sensors. *Macromolecules* **53**, 3709-3718 (2020).
34. Sun D, Lu T, Wang T. Nonlinear photoelasticity of rubber-like soft materials: comparison between theory and experiment. *Soft Matter* **17**, 4998-5005 (2021).
35. Arruda EM, Boyce MC. A 3-dimensional constitutive model for the large stretch behavior of rubber elastic-materials. *J. Mech. Phys. Solids* **41**, 389-412 (1993).
36. Arruda EM, Przybylo PA. An investigation into the 3-dimensional stress-birefringence-strain relationship in elastomers. *Polym. Eng. Sci.* **35**, 395-402 (1995).

37. Kuhn W, Grün F. Beziehungen zwischen elastischen Konstanten und Dehnungsdoppelbrechung hochelastischer Stoffe. *Kolloid-Zeitschrift* **101**, 248-271 (1942).
38. Es-Haghi SS, Offenbach I, Debnath D, Weiss RA, Cakmak M. Mechano-optical behavior of loosely crosslinked double-network hydrogels: Modeling and real-time birefringence measurement during uniaxial extension. *Polymer* **115**, 239-245 (2017).

Figures

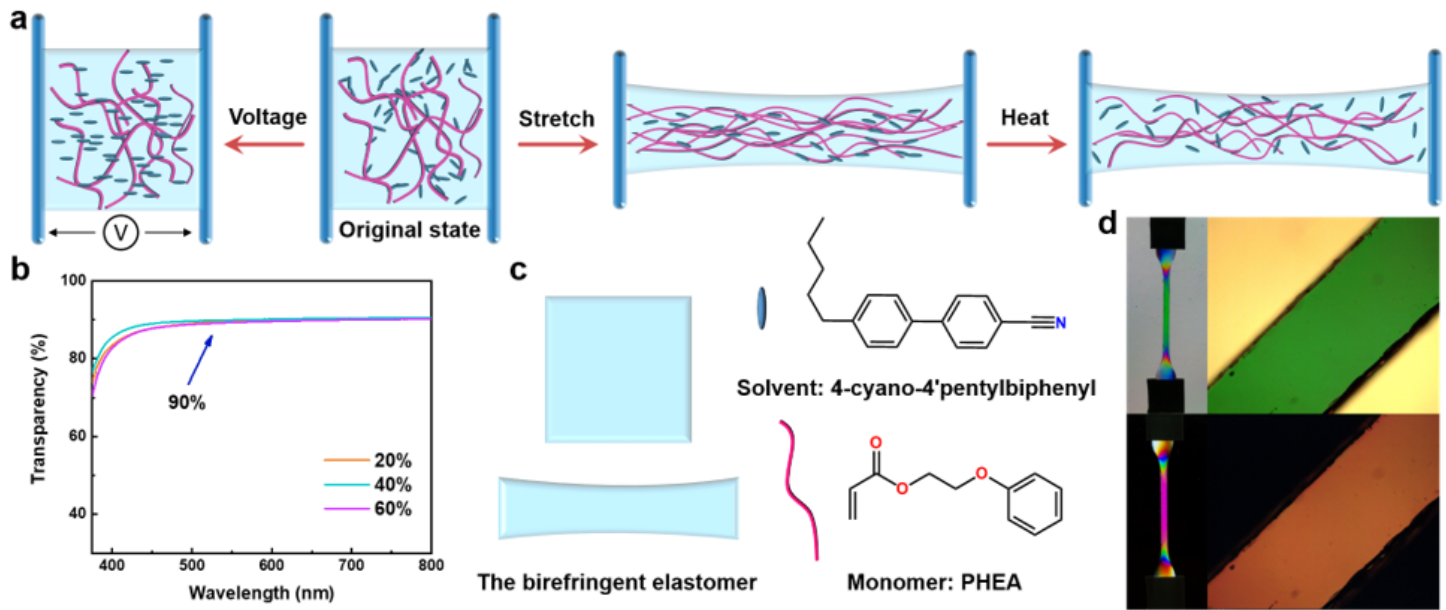


Figure 1

a) Schematic diagram of multiple stimuli-responsive birefringent elastomers. b) Transmittance of the birefringent elastomer in the wavelength range of 400-800 nm. c) The molecular structures of reactants used to fabricate the birefringent elastomer. d) Photos in bright and dark field and polarized light microscope photos of the birefringent elastomer.

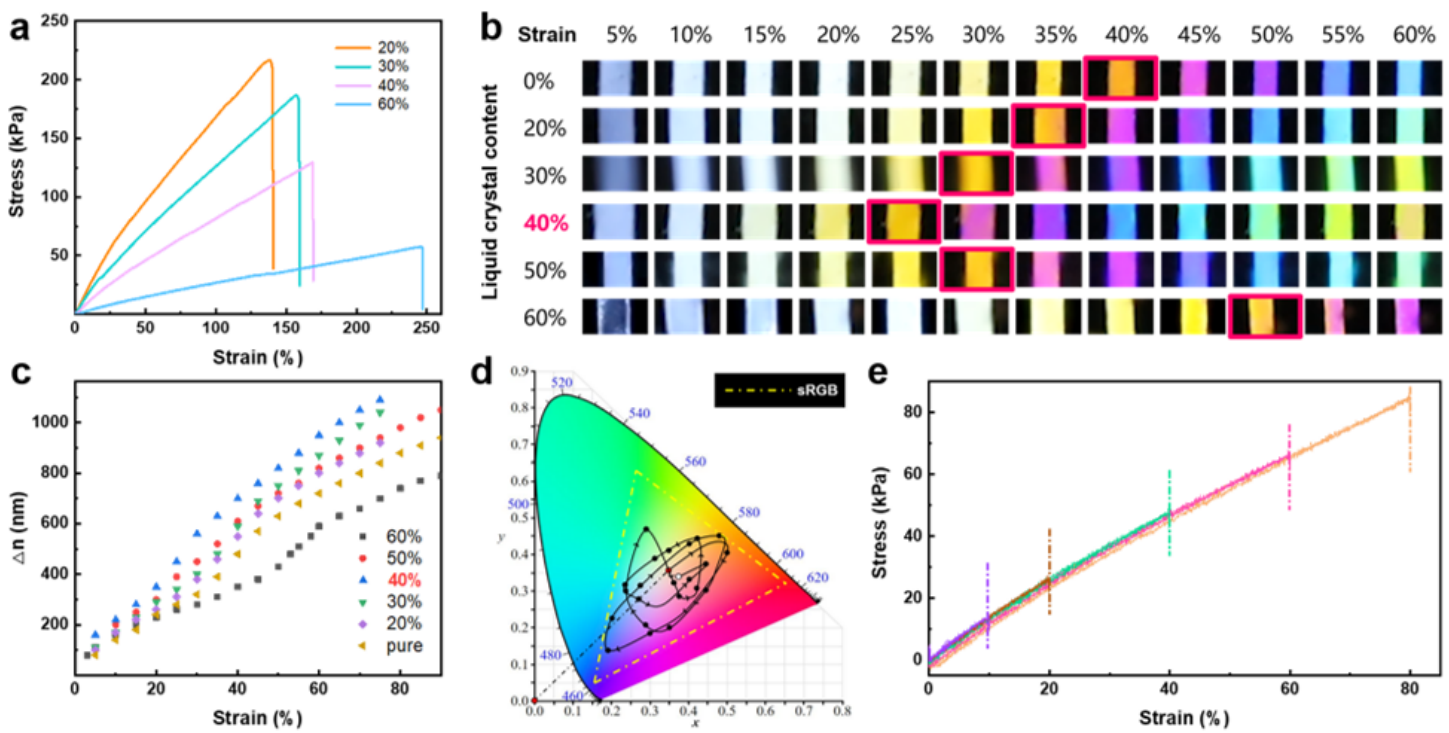


Figure 2

a) Stress-strain curve of the birefringent elastomers with different solvent contents. b) Correspondence between the elongation of the birefringent elastomer and interference colors. c) Curve of optical path difference (Δn) and strain. d) Color evolution during continuous stretching, presented at a standard CIE-1931 color space. The dotted line is the range of standard Red Green Blue (sRGB). e) Stretch recovery curve of the birefringent elastomer.

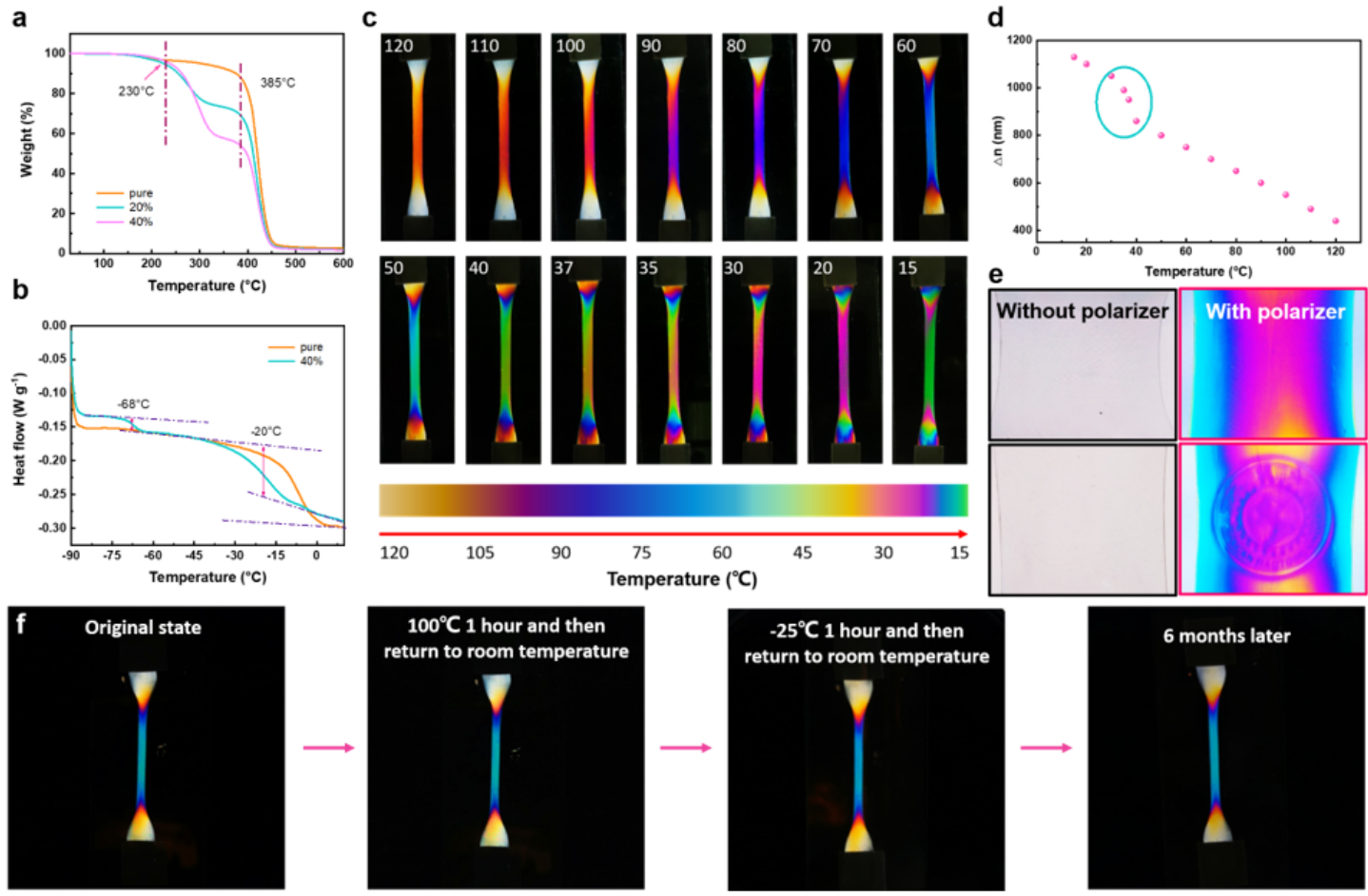


Figure 3

a) Thermogravimetric analysis (TGA) curves of the birefringent elastomer. b) Differential scanning calorimeter (DSC) curve of the birefringent elastomer. c). Correspondence between temperature of the birefringent elastomer and interference color. d) The curve of the optical path difference (Δn) of the sample with temperature. e) Write the emblem of Xi'an Jiaotong University into the birefringent elastomer by changing the local temperature. f) The stability test of the interference color (temperature and environment).

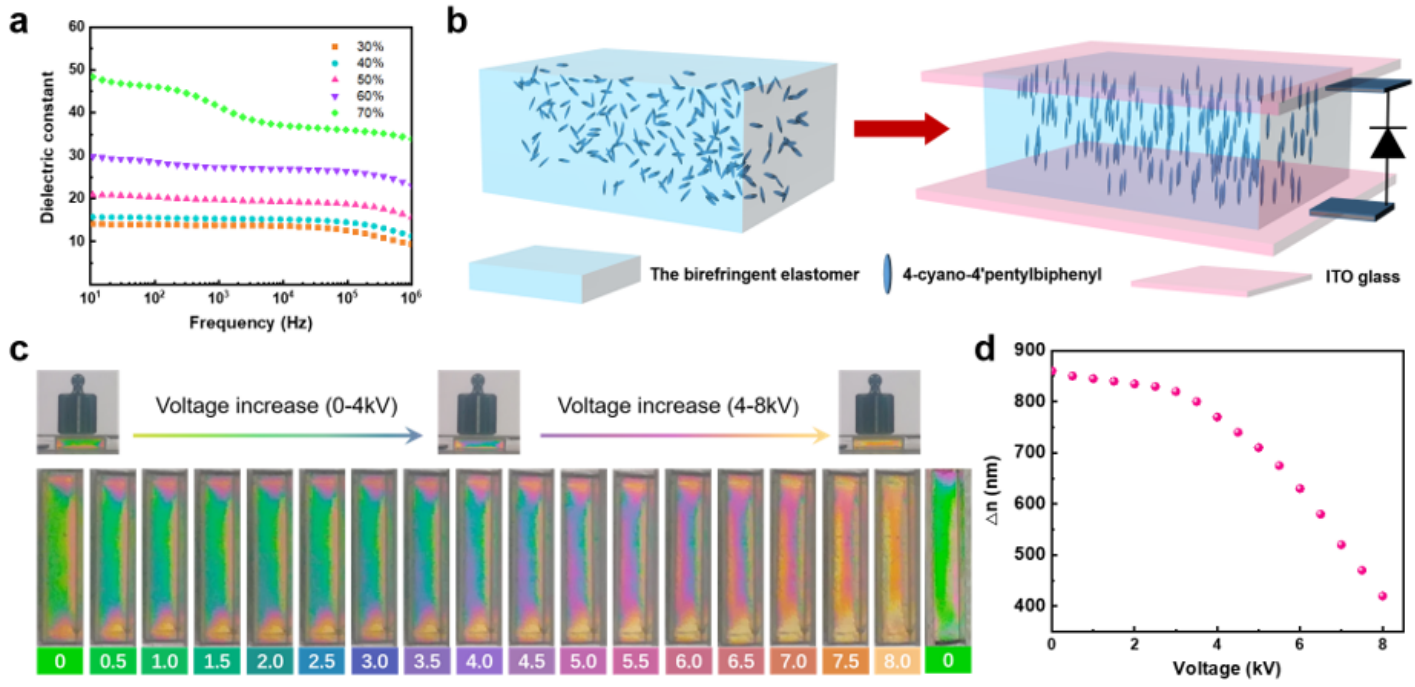


Figure 4

a) Plot of dielectric constants versus testing frequency for the birefringent elastomer. b) Schematic diagram of the orientation of solvent molecules in an electric field birefringent elastomer. c) Correspondence between the voltage applied on the birefringent elastomer and interference colors. d) The curve of the optical path difference of the sample with voltage.

Supplementary Files

This is a list of supplementary files associated with this preprint. Click to download.

- supporting1207.docx
- MOVIES1.mp4
- MOVIES2.mp4
- MOVIES3.mp4
- MOVIES4.mp4
- MOVIES5.mp4
- MOVIES6.mp4